Band offsets of ultrathin high-κ oxide films with Si

Eric Bersch, Sylvie Rangan, and Robert Allen Bartynski
Department of Physics and Astronomy and Laboratory for Surface Modification, Rutgers University, 136 Frelinghuysen Road, Piscataway, New Jersey 08854, USA

Eric Garfunkel
Department of Chemistry and Chemical Biology and Laboratory for Surface Modification, Rutgers University, 610 Taylor Road, Piscataway, New Jersey 08854, USA

Elio Vescovo
National Synchrotron Light Source, Brookhaven National Laboratory, Upton, New York 11973, USA
(Received 13 May 2008; published 12 August 2008)

Valence- and conduction-band edges of ultrathin oxides (SiO_2, HfO_2, $Hf_{0.7}Si_{0.3}O_2$, ZrO_2, and Al_2O_3) grown on a silicon substrate have been measured using ultraviolet photoemission and inverse photoemission spectroscopies in the same UHV chamber. The combination of these two techniques has enabled the direct determination of the oxide energy gaps as well as the offsets of the oxide valence- and conduction-band edges from those of the silicon substrate. These results are supplemented with synchrotron x-ray photoemission spectroscopy measurements allowing further characterization of the oxide composition and the evaluation of the silicon substrate contribution to the spectra. The electron affinity has also been systematically measured on the same samples. We find reasonably good agreement with earlier experiments where assumptions regarding energy-gap values were needed to establish the conduction-band offsets. The systematics of our photoemission and inverse photoemission results on different ultrathin films provide a comprehensive comparison of these related systems.

DOI: 10.1103/PhysRevB.78.085114 PACS number(s): 77.55.+f, 73.40.Qv, 82.80.Pv

I. INTRODUCTION

The continual scaling of metal-oxide-semiconductor field-effect transistors (MOSFET's) to smaller dimensions requires not only smaller area devices but a thinner oxide layer between the metal gate and the semiconductor channel in order to maintain high capacitance in the device. Historically, SiO_2 has been the oxide of choice because it forms an abrupt interface with Si that can be fabricated with an extremely low density of electrically active defects and thus allows high channel mobility. However, as the required thickness of SiO_2 extends below 1 nm, the resultant large leakage current that occurs across the oxide results in intolerably high power consumption and unacceptable heat loads. A recently successful approach to addressing these problems is to replace the SiO_2 gate oxide with an alternative dielectric that has a high dielectric constant (high κ). Such a structure maintains a high capacitance while lowering the leakage current. However, most high-κ dielectrics, such as HfO_2, ZrO_2, and their silicates, have much smaller band gaps than those of SiO_2. This property makes the alignment of the valence-band edges and conduction-band edges of the dielectric and semiconductor, as well as the alignment of the dielectric's band edges with the Fermi level of the metal gate, a critical issue. To maintain a low leakage current and small effective oxide thickness, large band offsets (at least 1 eV) with the silicon substrate at both the valence- and the conduction-band edges are required.[1,2]

Figure 1 schematically illustrates the alignment between conduction-band edges and valence-band edges for a high-κ dielectric film grown on a Si substrate.[3] Typically, when a high-κ dielectric is grown on Si, there is an unavoidable interfacial SiO_2 layer (5–10 Å). In our discussion, we will refer to the valence-band and conduction-band offsets of the high-κ material with respect to the silicon substrate band edges as the VBO and CBO, respectively. Another important parameter is the electron affinity of the oxide (χ), which is the energy difference between the measured bottom of the conduction band and the vacuum level. In general as the SiO_2 band gap is larger than that of most high-κ dielectrics, it is difficult to obtain direct information about the band edges of the interfacial SiO_2 layer. However, in most cases the SiO_2 layer is thin enough for electrons to tunnel through it, so that the most relevant band offsets are effectively the ones between the high-κ layer and the silicon substrate.

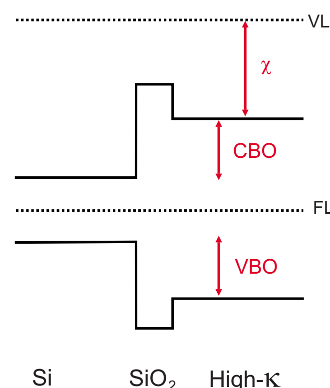

FIG. 1. (Color online) Schematic representation of band alignment across a high-κ/SiO_2/Si structure.

 ©2008 The American Physical Society

There have been a large number of studies aimed at determining band alignment between high-κ films and the underlying Si substrate. One class of measurement uses the electrical properties (*CV* and *IV*) of MOS test structures and extracts band offset information by modeling the electrical response. Such approaches usually assume an effective work function, a density of fixed charges in the dielectric and sometimes an interface dipole. Spectroscopic approaches to the band alignment problem have concentrated on photoconductivity (PC) and internal photoemission (IntPE) measurements, where the photon-induced current across an MOS device structure is measured as a function of photon energy. In these spectroscopies, it is exceedingly difficult to extract electronic structure information other than the band offsets, which themselves are not obtained directly from the raw photocurrent signal. Moreover, as these spectroscopies are based on electrical measurements, they require a metal overlayer on top of the oxide gate which can modify the properties of the stacks. In photoemission spectroscopy, the energy of spectroscopic features attributed to the valence-band edges of the semiconductor and the high-κ dielectric overlayer are compared to a common reference. In this way, it is possible to examine the valence-band offsets in a direct way. However, information about conduction-band offsets is not attainable as spectroscopic features in photoemission reflect the density of occupied electronic states.

Alternative spectroscopic approaches to determining the energy of the conduction-band edge in high-κ materials include x-ray absorption spectroscopy (XAS) and electron-energy-loss (EEL) features in core-level photoemission spectroscopy. In XAS, the optical absorption of a sample is measured as the photon energy is swept through the energy range for excitation of a core electron. Under favorable circumstances, the spectroscopic line shape in the near-edge region reflects the unoccupied density of states near the excited atom. However, as XAS arises from an optical transition, dipole selection rules enable one to probe only the density of unoccupied states with appropriate symmetry. In addition, as the excited atom contains a core hole, the density of states being probed could be modified from that of the ground state. Although electron-energy-loss spectroscopy (EELS) can in principle give a direct measurement of a gap, EEL features in core-level spectroscopy are notoriously weak, typically an order of magnitude or more weaker than the primary core-level photoemission feature, and broadened by lifetime effects. Moreover, the edge is riding on a background generated by other transitions in the spectrum, and the resolution is limited by lifetime broadening in the core-level spectrum.

While the above discussion does not attempt to address all possible methods of determining band offsets, efforts to determine both conduction-band (CB) and valence-band (VB) offsets typically require the use of parameters from the literature, such as the oxide band gap, to complement experimental results. This is of particular concern because for high-κ dielectric films, all of the properties of interest, the energy gap, the VBO, and the CBO, can vary as a function of sample preparation, including film growth technique, history of thermal treatment, and ultimately the quality of the film. Moreover, as high-κ dielectric films are notoriously sensitive to electron- and photon-beam effects, particular care must be exercised in obtaining spectroscopic information.

In this paper, we present the results of a combined ultraviolet photoemission spectroscopy (UPS) (to probe the occupied electronic state) and inverse photoemission spectroscopy (IPS) (to probe the unoccupied electronic states) study of a series of high-κ dielectric films grown on Si substrates. Our objective is to measure directly the band gap and band offsets (with respect to the substrate Si) of these films in a single experimental chamber. From these measurements, we can determine both the valence-band and conduction-band densities of states, as well as extract the electron affinity of the oxide film. In addition, we have performed synchrotron-excited soft x-ray photoemission studies of the same samples in an effort to characterize the shallow core levels of these systems and investigate the chemical state of the films and interface. We have also explored the role that factors such as sample charging and (photon- or electron-) beam effects have on the reliability and reproducibility of such spectroscopic measurements.

Measurements were performed on HfO_2, $Hf_{0.7}Si_{0.3}O_2$, ZrO_2, and Al_2O_3 high-κ dielectric films, as well as an SiO_2 film, for comparison. Our results are, in general, in good agreement with those found in the literature.

II. EXPERIMENTAL METHODS

A. Spectroscopic techniques

The majority of measurements presented here were obtained using a single ultrahigh vacuum experimental chamber that housed instrumentation for both UPS and IPS. The base pressure of the chamber was less than 5×10^{-10} Torr. Valence-band photoelectrons were excited using a Leybold Heraeus helium discharge photon source (He I: 21.2 eV; He II: 40.8 eV) and energy analysis of the emitted electrons was performed in an angle-integrated mode using a double-pass Phi 15-255G cylindrical mirror analyzer (CMA). The axes of the photon source and the CMA formed a 90° angle and the sample normal was oriented midway between the two. By applying a −5 V bias to the sample under exposure to He I radiation, the entire width of the photoemission spectrum could be measured and the binding energy of the valence-band maximum (VBM) with respect to the vacuum level determined. From this information and a direct measurement of the energy gap, the electron affinity (χ) of the oxide was determined.

Inverse photoemission spectra were obtained using a grating spectrometer, described elsewhere,[4] which was mounted on the same experimental chamber. Briefly, a well-collimated beam of monoenergetic electrons (either at 20.3 or 23.3 eV in this study) was directed toward the sample along the surface normal. The electrons couple to high-lying unoccupied states and a subset relax via a direct optical transition to low-lying unoccupied states in the conduction band, emitting a photon in the process. The photons were dispersed by a concave spherical diffraction grating and detected by a microchannel plate with position sensitive resistive anode encoder. With this approach, the intensity of photons as a function of photon energy reflects the density of unoccupied

states in the conduction band. Moreover, as both the incident electron energy and the range of measured photon energy can be varied with this instrumentation, cross-section effects can be used to improve spectra analysis. In contrast to our UPS measurements, IPS spectra obtained with a well-collimated electron beam, such as that employed here, are in principle momentum resolved and for single-crystal samples would probe a very restricted portion of the bulk Brillouin zone of the sample. In our case, however, the high-κ films are essentially amorphous or polycrystalline and thus our gap measurements are unaffected. VB and CB are both calibrated using the Fermi level of a gold sample. The overall energy resolution for the UPS and IPS is estimated to be ± 0.1 eV.

Shallow core-level and valence-band photoemission spectroscopy have also been performed on the U5UA beamline at the National Synchrotron Light Source.[5] Photoelectrons were collected with an Omicron 125 mm hemispherical electron-energy analyzer with an angular resolution of $\pm 1°$ oriented along the sample normal. The photon beam impinged on the sample at an angle of 45°. Spectra were taken at a 150 eV photon energy, with an instrumental energy resolution of 0.1 eV. The pressure in the analysis chamber was always better than 1×10^{-10} Torr. The position of the core levels was calibrated using the Fermi level measured on a silver foil that was in electrical contact with the sample.

Electron spectroscopic measurements of large gap oxides is challenging owing to constant concern about energy shifts or broadening owing to sample charging. To minimize these effects in this study, all of our samples consisted of thin oxide layers (15–30 Å) and great care has been taken to evaluate the charging effects in UPS and IPS. A sequence of short ($\sim$30 s) scans, during which no charging could be detected, alternated with short ($\sim$1 min) 600 °C anneals between scans, as well as low photon and electron fluxes, were enough to prevent or compensate for charging in our UPS and IPS work. For the synchrotron-excited core-level spectroscopy, no evidence of charging was observed. At least two samples, obtained from the same Si wafer, were measured for each dielectric. The difference obtained for each sample, with the same preparation conditions, was at most 0.1 eV, which is within our overall experimental resolution. Note that owing to the different doping of the silicon substrates used for oxide growth in this work, we have chosen to refer all x-ray photoemission spectroscopy (XPS), UPS, and IPS spectra with respect to the midgap position of silicon (taken as 0.6 eV above the silicon valence-band maximum).

B. Sample treatment

All of the dielectric films measured in this study were grown on single-crystal Si(100) surfaces and transported in air to our spectroscopy chambers. Thin films in the thickness range of 15–30 Å of HfO_2, $Hf_{0.7}Si_{0.3}O_2$, SiO_2, ZrO_2, and Al_2O_3 were examined. Details regarding film preparation are outlined in Sec. III. Upon insertion into the experimental chamber, the samples were cleaned by resistive heating to about 600 °C for several minutes. This treatment has proved to be critical in order to avoid the appearance of spectral features within the band gap of the dielectric during measurements, most likely owing to reaction between adsorbed species and the dielectric film that were induced by the IPS electron beam. An example of this effect is shown in Fig. 2 for a 15 Å HfO_2 film grown on Si. The black curves in Fig. 2 are a UPS spectrum of the VB and an IPS spectrum of the CB. For display purposes, the maximum intensities of these curves were normalized to the same height. The UPS spectrum of the valence band shows a sharp rise near −4 eV, associated with the onset of the O $2p$ levels of the HfO_2 valence band. Similarly, the IPS spectrum of the conduction band shows a sharp increase near 2 eV associated with the location of the HfO_2 conduction-band maximum (CBM). However, as indicated by the red spectra, when the sample is exposed to a low-energy electron beam (about 20 eV) prior to annealing, spectroscopic intensity appears between the valence-band and conduction-band edges of the dielectric. As further annealing does not remove this intensity, we attribute it to electronic states induced by an irreversible reaction of adsorbed species with the oxide surface. In our studies, the samples were always well degassed before any spectroscopic measurements were attempted. Furthermore, we followed a measurement sequence of performing UPS, followed by IPS, followed by a second UPS spectrum to ensure that the IPS electron beam did not induce any spectroscopic changes to the sample.

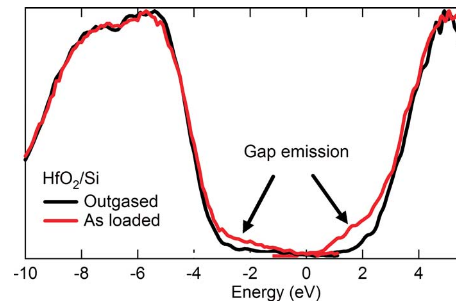

FIG. 2. (Color online) Valence bands and conduction bands of two 15 Å HfO_2/Si samples obtained respectively using UPS and IPS, with and without outgassing. Annealing in UHV prevents gap emission from appearing when a sample is exposed to a low-energy electron beam (about 20 eV). The spectra are referred to the midgap of silicon.

Another concern when working with oxides is the chemical reduction of the oxide surface region during UHV annealing or under an incident electron beam (e.g., when acquiring Auger electron spectra). We did not find any noticeable changes during our XPS, UPS, and IPS measurements. The intensity ratio of the O $2s$ core level to either Hf $4f$, Si $2p$, Zr $4p$, or Al $2p$ core level was monitored upon anneals and during photon-beam exposure and remained unchanged. We also annealed our samples to higher temperatures in order to create visible stoichiometric or structural changes, as monitored by changes in core level or valence-band line shape. We saw no modification of the spectra until temperatures well above the value of 600 °C used in this study.

C. Band-edge determination

Experimental spectra from oxide films grown on silicon substrates often exhibit spectral intensity in the energy range

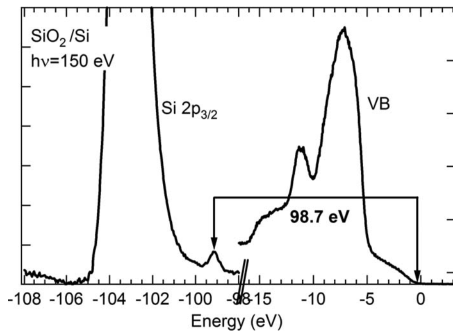

FIG. 3. Si $2p$ core level and valence band for SiO_2 on silicon. The Si $2p_{1/2}$ contribution has been removed assuming a 0.6 eV spin-orbit splitting and 0.5 Si $2p_{1/2}$ to Si $2p_{3/2}$ ratio. The spectra are referred to the midgap of silicon.

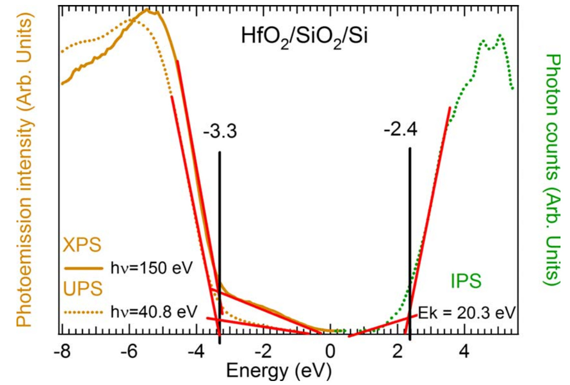

FIG. 4. (Color online) UPS and IPS spectra of a 15 Å HfO_2/10 Å SiO_2/Si sample. Band edges are obtained after subtraction of the linearly extrapolated silicon background. The band edges' positions are indicated.

of the oxide band gap. It is critical to determine whether such emission is: (a) associated with bona fide band-gap states associated with imperfections in the oxide film (which can have important implications for its electrical performance),[6] (b) caused by the reaction of adsorbed species with the film as mentioned above, or (c) simply emission from the Si substrate on which the film was grown. We want to clarify this point for our spectra.

Figure 3 shows a soft x-ray spectrum obtained from a well degassed sample comprised of a 20 Å film of SiO_2 grown on the Si(100) surface obtained with a photon energy of 150 eV. The valence band is shown as well as the bottom part of the Si $2p_{3/2}$ component of the core level. (Here the contribution from the Si $2p_{1/2}$ component has been removed from all oxidation states assuming a 0.6 eV spin-orbit splitting and a Si $2p_{1/2}$ to Si $2p_{3/2}$ ratio of 0.5.) A weak but sharp feature at −99.2 eV shows the Si $2p_{3/2}$ line associated with Si^0 atoms in the underlying semiconductor substrate. Similar to the UPS spectrum in Fig. 2, the valence band shows a sharp rise at ∼5 eV associated with the oxide valence-band minimum. In contrast to the clean spectrum in Fig. 2 however, this VB spectrum exhibits substantial intensity to a binding energy of ∼0.5 eV. The energy difference between the onset of valence-band emission at ∼0.5 eV and the location of the Si^0 peak is precisely the energy difference between the Si $2p_{3/2}$ core level and the VB edge of elemental Si.[7] This is strong evidence that the emission in the oxide band gap observed for this system is not associated with defects in the oxide film or at the oxide/Si interface but rather is simply emission from the underlying Si substrate.

In our XPS, UPS, and IPS spectra, the use of thin dielectric films results in contributions from both the valence and conduction bands of the substrate Si. To determine the band edge of the dielectric, we account for this extra emission by assuming a linear contribution from the silicon substrate. While in principle it might be preferable to subtract the appropriately scaled line shape of the elemental Si valence band, typically the substrate contribution is so small that a linear assumption does not introduce a significant error.

An example of this procedure is illustrated in Fig. 4, which contains XPS and He II UPS spectra of the valence band and IPS spectra of the conduction band (with intensity maxima normalized to the same height) from a 15 Å HfO_2 film on Si(100). The zero of energy is referenced to the silicon midgap. For samples excited by He II radiation ($h\nu = 40.8$ eV), the contribution to the photoemission spectrum from the substrate silicon valence band is extremely small and ignoring it would not lead to significant error. Simplifying matters, the rapidly rising edge emission from the HfO_2 oxygen $2p$ states is also well fitted with a linear function. We define the HfO_2 valence-band edge as the intersection of the fit to the silicon substrate with the fit to the more obvious HfO_2 edge. This fitting procedure, applied to the XPS or UPS valence-band spectra, gives the same result for the edge position (with an error estimated to be ±0.1 eV, comparable to the experimental error of the energy scale). Here we measure the HfO_2 valence-band edge at 3.3 eV below the silicon midgap. On the CB side, the contribution of the substrate is relatively more significant and thus the fit is needed to avoid significant error (about 0.3 eV). The oxide CB edge is found 2.4 eV above the silicon midgap. Using this procedure to obtain the energy of the band edges, the oxide gap is measured to be 5.7 eV.

When the sample is excited by 150 eV photons, electrons ejected from the valence band have kinetic energies in the range of ∼135–145 eV. In contrast, Si $2p$ core-level photoelectrons are ejected with kinetic energies in the range of 50 eV. Owing to the different inelastic mean free paths for electrons in these two kinetic energy ranges, the valence-band portion of the photoemission spectrum is more bulk sensitive than the Si $2p$ core-level region is. As the silicon substrate is buried 15–30 Å beneath the oxide surface, even when the valence band of the underlying silicon is visible, the Si $2p$ core level is often a very weak spectral feature and does not always allow precise determination of the amount of band bending in the Si.

In this study, the valence- and conduction-band offsets are extracted from the oxides band edges and from the silicon valence-band position, measured as described above. In most cases, the position of the Fermi level measured experimentally on a metallic sample in contact with the high-κ/Si stacks was different from its expected position based on the known resistivity of our silicon substrates. This apparent downward band bending in the silicon substrate will be discussed later.

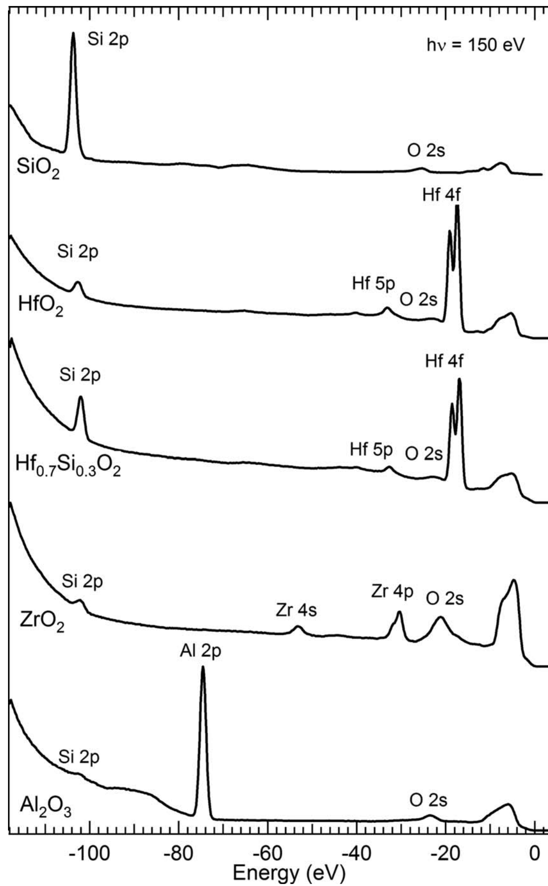

FIG. 5. XPS survey spectra for the different dielectric films examined in this study.

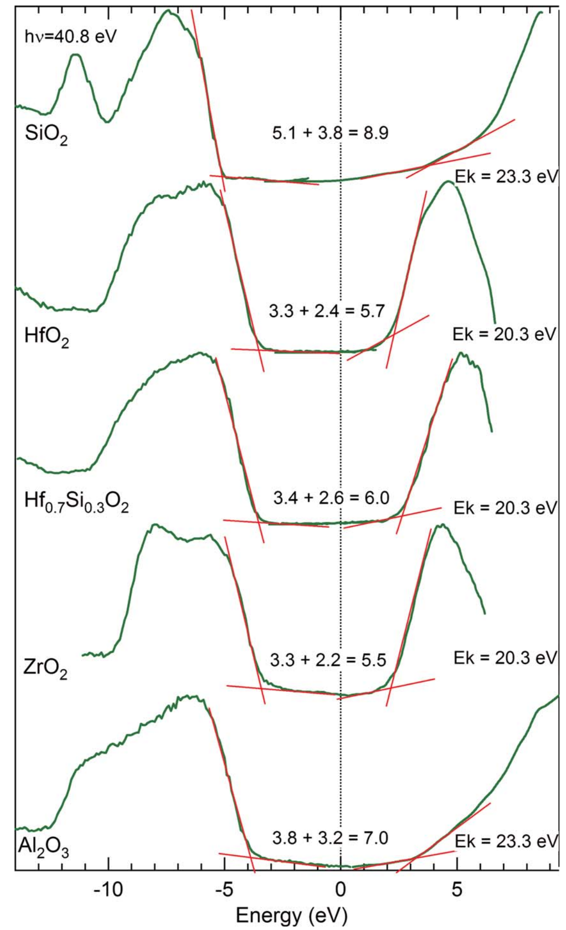

FIG. 6. (Color online) The valence and conduction bands of the different dielectrics have been measured in the same UHV system. The photon energy used for UPS and the incident electron kinetic energy used for IPS are indicated. The positions of the valence- and conduction-band edges with respect to the midgap of silicon are indicated.

Electron affinity (χ) measurements have also been performed using the He I UV source with a -5 V bias on the sample. The total width of the spectrum, W, is extracted using a linear extrapolation of the data to the background intensity level at both the high- and low-kinetic-energy ends of the spectrum. The electron affinity is then obtained as

$$\chi = h\nu - W - E_{\text{gap}}, \tag{1}$$

where $h\nu$ is the photon source energy and E_{gap} is the experimentally measured gap of the high-κ dielectric film.

III. RESULTS AND DISCUSSION

A. Overview

Figure 5 contains a series of soft x-ray photoemission survey spectra obtained from each of the samples studied in this work. Oxide valence-band features and core-level lines from the dielectric are evident. The Si $2p$ core-level region is dominated by a peak at $\sim$103.7 eV, which is indicative of Si in the 4+ oxidation state and is characteristic of the SiO_2 interfacial layer or of the dielectric overlayer in the case of SiO_2. The relative intensity of this peak varies from spectrum to spectrum for several reasons. For the SiO_2 sample, clearly Si^{4+} ions are present up to the surface and thus a large intensity is expected. The HfO_2 and $Hf_{0.7}Si_{0.3}O_2$ films are both $\sim$15 Å thick, but the spectrum from the silicate shows a larger Si $2p$ core level because, once again, there is Si throughout the film. The Si $2p$ peak is particularly weak in the ZrO_2 spectrum as the thickness of this film is $\sim$24 Å, significantly larger than those of the hafnium-based films. In the Al_2O_3 case, the film is again $\sim$24 Å. However the Si $2p$ core level appears smaller owing to a combination of rescaling to accommodate the intense Al $2p$ core-level feature and because the Al $2p$ line generates a significant background of inelastically scattered electrons. In addition to the Si core level, the spin-orbit-split Hf $4f$ doublet is clearly visible, as are the Hf(Zr) $5p(4p)$ and Zr $4s$ levels. These oxide core levels will be useful in establishing oxidation and chemical states in our subsequent discussion. Finally, while the O $2s$ feature is present in all spectra, it is nearly overwhelmed by the Hf $4f$ levels in the Hf-containing compounds and will not be used extensively in our analysis. In our discussion below, we will examine these core levels in detail, particularly with regard to their energy separation from valence-band features.

Figure 6 shows the UPS and IPS spectra of the valence-band and conduction-band regions, respectively, of the five dielectric films measured in this work. For all spectra, the zero of energy has been aligned with the midgap of the sili-

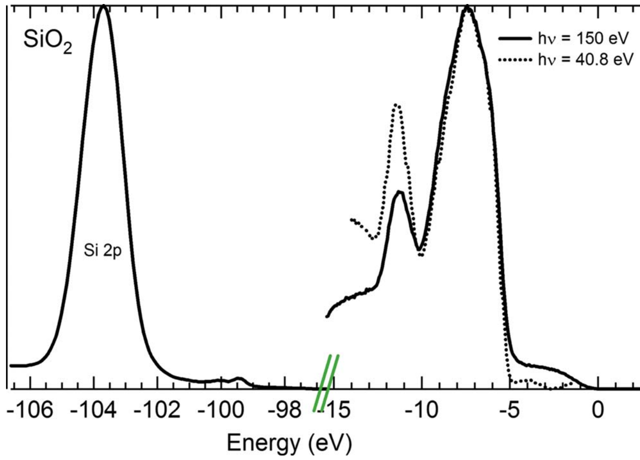

FIG. 7. (Color online) Si 2p core level and valence band measured at 150 eV photon energy (continuous line) and the valence band measured at 40.8 eV photon energy (dotted line) from SiO_2/Si. The zero of binding energy is referenced to the Si substrate midgap position.

con substrate. While all of the photoemission spectra show a strong rising edge near 4 eV binding energy associated with the O 2p levels of the dielectric, the IPS spectra show more variation. A strong edge is seen at about 2 eV above the Fermi level for the Hf- and Zr-containing compounds, while the increase in intensity corresponding to the conduction-band minimum is less obvious for SiO_2 and Al_2O_3. This is primarily owing to the presence of unoccupied Hf 5d or Zr 4d levels in the transition-metal compounds. These levels have a large cross section for optical transitions in the energy range used in these experiments. In contrast, the conduction bands of SiO_2 and Al_2O_3 are comprised primarily of Si or Al 4s and 3p orbitals, which exhibit much weaker transitions.[8,9] The linear fits used to determine the VBM and CBM in each case is shown in Fig. 6, and the energies of these edges with respect to the silicon midgap, as well as the resultant measured band gaps, are indicated. In Secs. III B and III F, these spectra and their relationship to those obtained with soft x-ray synchrotron radiation are discussed.

B. SiO_2

The SiO_2 sample used in this study was a 20 Å thermal oxide grown on an n-doped Si with a resistivity of 70 Ω cm^{-1}, which places the Fermi level of the substrate 0.78 eV above the Si valence-band maximum. The measured Fermi level is found 0.7 eV above the silicon valence band, which given our experimental error of 0.1 eV on the energy scale is close to the value of the substrate.

The soft x-ray excited photoemission spectrum from the SiO_2 sample, shown in Fig. 5, indicates the relative intensity of the Si 2p core level and the VB emission: A strong and well defined peak at 103.7 eV, which is characteristic of the 2$p_{3/2}$ core level of Si^{4+}, dominates the spectrum so that the SiO_2 valence band appears artificially small. Also shown in Fig. 7 is the valence band obtained at 150 eV photon energy compared to the valence band obtained with He II radiation at 40.8 eV photon energy (dashed curve), rescaled in intensity so that the low-binding-energy peaks coincide. This comparison re-emphasizes that the valence-band spectrum obtained by UPS is more surface sensitive than the soft x-ray one, so that the underlying silicon contribution is essentially absent.

TABLE I. Literature values for SiO_2 band gap and SiO_2-Si VBO and CBO in eV.

Method	Gap	VBO	CBO
XPS, energy loss[a]	8.95	4.49	3.34
XPS, UPS[b]	9.0	4.4	3.5
IntPE[c]			3.15
XPS[d]		4.35	
XPS[e]	8.95	4.54	3.28
SE[f]	8.90		
This work	8.9	4.5	3.3

[a]Reference 11.
[b]Reference 14.
[c]Reference 15.
[d]Reference 13.
[e]Reference 12.
[f]Reference 16.

The SiO_2 valence band (Fig. 7), primarily of O 2p character,[10] possesses a sharp edge on the high-energy side, and the position of the valence-band maximum is easily determined to be 5.1 eV with respect to the silicon midgap. Given the position of the Si VB at −0.6 eV, the SiO_2/Si valence-band offset is 4.5 eV. As mentioned above, the conduction band is a mixture of Si 4s and Si 3p contributions and, rather than being composed of a single abrupt edge, exhibits two intensity changes with different slopes. The IPS spectrum of SiO_2/Si shown in Fig. 6 displays an initial linear increase attributed to emission from the Si substrate, then an additional change in slope near 4 eV, followed by a more significant rise at ~6 eV as indicated by the straight line fits in Fig. 6. After subtraction of the substrate contribution, the SiO_2 conduction-band edge is located 3.8 eV above the Fermi level, giving a gap of 8.9 eV. With respect to the Si CBM, the SiO_2/Si conduction-band offset is calculated to be 3.3 eV. These quantities are compared to previously quoted values from the literature that were obtained using different methods including XPS,[11–14] energy loss,[11] IntPE,[15] and spectroscopic ellipsometry (SE) in Table I. By measuring the width of the photoemission spectrum from a biased sample using He I radiation, the electron affinity of this SiO_2 film is measured to be 1.3 eV.

C. HfO_2

The HfO_2 sample studied here was 15 Å thick and was grown at IBM by atomic layer deposition (ALD) on a p-doped Si with a resistivity of 1–2 Ω cm^{-1}. This places the Fermi level of the Si substrate at 0.22 eV above the valence-band maximum. Our spectroscopic data were complemented with medium-energy ion scattering (MEIS) measurements (not shown) which found a slightly oxygen-rich composition for the film ($HfO_{2.15}$) as well as a 10 Å SiO_2 interfacial layer. The measured Fermi level was found 1.0 eV above the silicon valence band, indicating a strong band bending in the silicon substrate.

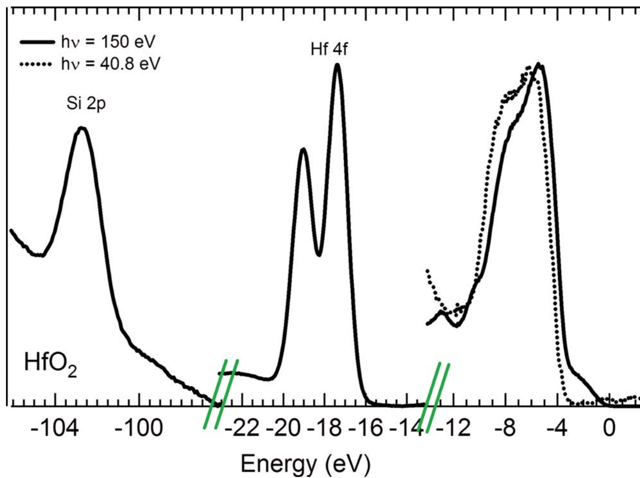

FIG. 8. (Color online) Si 2p and Hf 4f core levels and valence band measured at 150 eV photon energy (continuous line) and the valence band measured at 40.8 eV photon energy (dotted line) from HfO_2/Si. The zero of binding energy is referenced to the Si substrate midgap position.

The soft x-ray survey scan in Fig. 5 shows that the Hf 4f core-level emission dominates the photoemission spectrum. For this sample, no signal from the silicon bulk was visible as the total oxide thickness (hafnia+interfacial oxide) was 25 Å, compared to 20 Å for the SiO_2 sample. In the XPS spectrum in Fig. 8 the Si 2p peak from this sample, at 102.6 eV below the silicon midgap, is shifted to slightly lower binding energies than what was found for the pure SiO_2 film. These low-binding-energy features are associated with Si suboxides at the interface between the silicon substrate and the HfO_2. The Hf 4f contribution to the spectrum is from the Hf $4f_{5/2}$ and Hf $4f_{7/2}$ core levels, which can be fitted with two Voight line shapes at 19.2 and 17.5 eV, respectively, both with an energy width of 1.0 eV (1.0 eV Gaussian and 0.2 eV Lorentzian). These values are comparable to those previously reported in the literature.[17]

The electronic structure of HfO_2 is characteristic of a transition-metal oxide. The valence band is primarily of O 2p character (with a small admixture of Hf 5d character). Similar to the case for the SiO_2, under excitation by He II radiation, there is essentially no substrate emission observed in the energy range of the dielectric band gap. A linear fit to the high-energy side of the valence emission puts the valence-band edge at 3.3 eV below the Fermi level. Given the position of the substrate VB, the HfO_2/Si VBO is calculated to be 2.7 eV. In contrast to the valence band, the IPS spectrum shows some intensity attributable to the substrate. However, the oxide conduction band is dominated by Hf 5d states, resulting in an onset of intensity whose edge, when the Si contribution is removed, is determined to be 2.4 eV above the Fermi level. This value gives a CBO with silicon of 1.9 eV and a band gap of 5.7 eV (Fig. 6).

In Table II, the VBO, CBO, and band-gap results for HfO_2 that we obtain here are compared to values reported in the literature. A quick scan of the table makes it clear that the experimental values quoted for HfO_2 are much more scattered than the accepted values for SiO_2. One reason for this is that we found the values one obtains for both the band gap and the band offsets are sensitive to the thickness of the HfO_2 film. Measurements we obtained from 30 Å HfO_2 films gave slightly larger gaps of 6.0 eV with VBO's and CBO's of 4.1 and 1.9 eV, respectively. Different growth methods for 15 Å films [ALD with O_3 precursor, ALD with H_2O precursor, and metal-organic chemical-vapor deposition (MOCVD)] gave similar values for the band gap and the band offsets as long as the film composition was the same. On the other hand, thermal treatment, particularly to high enough temperature to crystallize the film, can change the values as well. By measuring the width of the photoemission spectrum from a biased sample using He I radiation, the electron affinity of this HfO_2 film is measured to be 2.5 eV.

TABLE II. Measured values for HfO_2 band gap and HfO_2-Si VBO and CBO in eV.

Method	Gap	VBO	CBO
XPS, energy loss[a]	5.7	3.10	1.48
XPS, energy loss[b]	5.25	2.22	1.91
XPS, IPS[c]	5.86	3.28	1.46
XAS, XPS[d]	5.1	3.0	1.0
UPS[e]		2.75	
IntPE[f]	5.6	2.5	2.0
XAS[g]	6.0		≥1.2
EELS[h]	5.8		
SE[i]	5.8		
SE[j]	5.56		
This work	5.7	2.7	1.9

[a]Reference 18.
[b]Reference 19.
[c]Reference 20.
[d]Reference 21.
[e]Reference 22.
[f]Reference 23.
[g]Reference 24.
[h]Reference 25.
[i]Reference 26.
[j]Reference 27.

D. $Hf_{0.7}Si_{0.3}O_2$

Similar to the HfO_2 film described above, the $Hf_{0.7}Si_{0.3}O_2$ sample studied here was 15 Å in thickness and was grown at SEMATECH by ALD on p-doped Si with a resistivity of 1–2 $\Omega\,cm^{-1}$. With these parameters, the substrate Fermi level is 0.22 eV above the Si VBM. The measured Fermi level however is found 1.1 eV above the silicon valence band, indicating once again a downward band bending in the silicon substrate. This film also was characterized using MEIS and the results (not shown) indicate a slightly oxygen-rich composition for the film ($Hf_{0.7}Si_{0.3}O_{2.15}$) and a thin SiO_2 interfacial layer (~5 Å).

The survey spectrum at 150 eV photon energy in Fig. 5 shows that, although this hafnium silicate film has the same thickness as the HfO_2 sample, the Hf 4f to Si 2p ratio has clearly decreased. Close-up spectra of the Si 2p and Hf 4f core levels and the VB of the silicate are shown in Fig. 9. The centroid of the Si 2p oxide peak is shifted toward lower binding energies at 102.1 eV (referenced to the silicon midgap) as a consequence of the silicon hafnium intermixing.

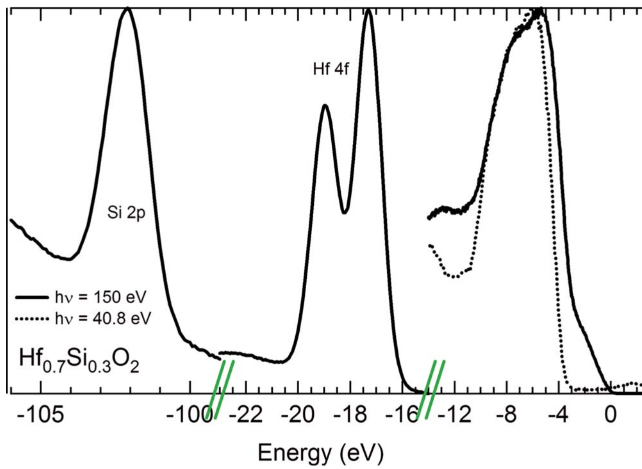

FIG. 9. (Color online) Si $2p$ and Hf $4f$ core levels and valence band measured at 150 eV photon energy (continuous line) and the valence band measured at 40.8 eV photon energy (dotted line) from $Hf_{0.7}Si_{0.3}O_2/Si$. The zero of binding energy is referenced to the Si substrate midgap position.

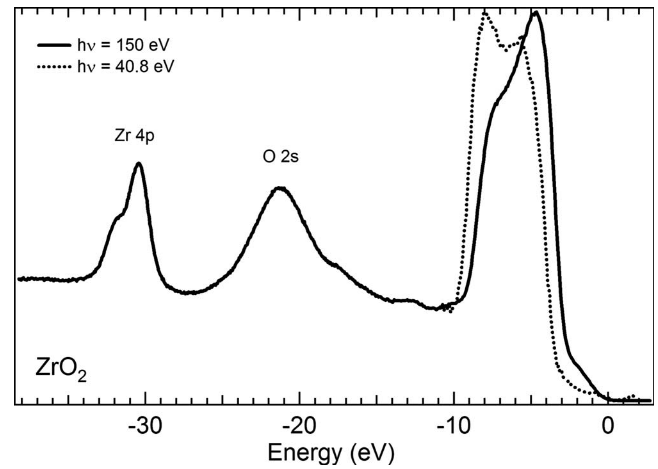

FIG. 10. Zr $4p$ core level and valence band measured at 150 eV photon energy (continuous line) and the valence band measured at 40.8 eV photon energy (dotted line). The zero of binding energy is referenced to the Si substrate Fermi level.

The Hf $4f_{5/2}$ and Hf $4f_{7/2}$ core levels can be fitted by Voight line shapes centered at 19.1 and 17.4 eV, respectively, with a 1.0 eV width (1.0 eV Gaussian and 0.2 eV Lorentzian). This value is close to the HfO_2 position and is still in good agreement with previous measurements of similar hafnium-rich silicates.[17] Despite the proximity of the Si ions, the core Hf $4f$ level is expected to be shifted toward higher binding energies by less than 0.1 eV at 102.1 eV (referenced to the silicon midgap).[17]

The $Hf_{0.7}Si_{0.3}O_2$ electronic structure can be compared to that of SiO_2 and HfO_2. Its valence band is of O $2p$ character and its shape is not too different from that of HfO_2, just slightly shifted toward higher binding energy to 3.4 eV. Compared to SiO_2, the conduction-band edge of $Hf_{0.7}Si_{0.3}O_2$ has a sharp edge characteristic of the Hf $5d$ contribution and is found at 2.6 eV. The gap value is found between the two limits SiO_2 and HfO_2 as 6.0 eV.

By obtaining a UPS spectrum using He I radiation and a sample bias of −5 eV, we find the width of the photoemission spectrum from the $Hf_{0.7}Si_{0.3}O_2$ sample to be 12.0 eV. Taking into account the band energies detailed above, the electron affinity of our $Hf_{0.7}Si_{0.3}O_2$ sample is determined to be 2.8 eV.

E. ZrO_2

While it is useful to compare the band offsets and band gaps of the hafnium silicate to that of the limiting cases of pure hafnium oxide and pure silicon dioxide, it is also important to place our band data in the context of other high-κ dielectric materials. In this spirit, we also measured the electronic structure of a 24 Å ZrO_2 film that was grown by ALD on a p-doped Si with a resistivity of 0.018 $\Omega\,cm^{-1}$. This doping places the bulk Si Fermi level 0.16 eV above the valence-band maximum, while the measured Fermi level was found 0.9 eV above the silicon VB. MEIS measurements (not shown) have found good stoichiometry for the dielectric film and revealed the presence of a 10 Å SiO_2 interfacial layer (with possibly some ZrO_2/SiO_2 mixing at the interface).

Figure 10 shows (solid curve) a closeup of the valence band and shallow core-level region of the ZrO_2 soft x-ray spectrum in Fig. 5. The He II UPS spectrum of the valence band is shown as the dashed curve. The Zr $4p$ feature can be deconvoluted into two Voight lines (both components having an energy width of 1.4 eV Gaussian and 0.2 eV Lorentzian) attributed to the Zr $4p_{1/2}$ and Zr $4p_{3/2}$ components at 32.0 and 30.4 eV, respectively, in good agreement with previous work.[28]

Similar to HfO_2, the valence band of ZrO_2 is mainly of O $2p$ character with a small Zr $4d$ contribution. As was observed for the $Hf_{0.7}Si_{0.3}O_2$ spectrum, a significant contribution from the substrate silicon produces an apparent shift of emission from the dielectric valence band in the soft x-ray spectrum to higher energy. Subtraction of the substrate intensity enables a consistent fit to the valence-band edge of both spectra, placing it 3.3 eV below the silicon midgap, giving a VBO of 2.7 eV. The conduction band is strongly Zr $4d$ in character and a clear edge position is fitted to 2.2 eV, giving a CBO of 1.7 eV.[29] Table III compares these results to other values quoted in the literature. Once again, by measuring the width of the photoemission spectrum from a biased sample using He I radiation, the electron affinity of this ZrO_2 film is measured to be 2.7 eV.

F. Al_2O_3

As a final comparison to an alternative high-κ dielectric, we performed direct and inverse photoemission measurements of a 25 Å thick Al_2O_3 sample grown by ALD on a p-doped Si with a resistivity of 0.006 $\Omega\,cm^{-1}$. Here the bulk Si Fermi level should be 0.07 eV above the valence-band maximum, while the measured Fermi level was found 1.0 eV above the silicon valence-band maximum. The thickness of the interfacial SiO_2 oxide layer has not been measured in MEIS but can be estimated to be at least 10 Å by comparing

TABLE III. Measured values for ZrO_2 band gap and ZrO_2-Si VBO and CBO in eV.

Method	Gap	VBO	CBO
XPS, energy loss[a]	5.65	3.65	0.88
XPS, energy loss[b]	5.50	3.35	1.03
XPS, energy loss[c]	5.6	2.5	2.0
XPS, UPS[d]	5.7	3.4	1.2
XPS, IPS[e]	5.68	3.40	1.16
IntPE[f]	5.4	2.3	2.0
EELS[g]	5.0		
SE[h]	5.25		
This work	5.5	2.7	1.7

[a]Reference 30.
[b]Reference 11.
[c]Reference 31.
[d]Reference 14.
[e]Reference 28.
[f]Reference 15.
[g]Reference 25.
[h]Reference 32.

the Si $2p$ peak height measured in the survey spectrum at 150 eV photon energy for Al_2O_3 with samples for which the thickness is known (Fig. 5). The Al $2p$ peak shown in Fig. 11 is comprised of two components, the Al $2p_{3/2}$ and Al $2p_{1/2}$ lines, found at binding energies of 74.4 and 74.8 eV, respectively, with a 1.3 eV Gaussian and 0.2 eV Lorentzian contribution for the width, in good agreement with previous work.

The electronic structure of the valence and conduction bands of Al_2O_3 is very similar to that of SiO_2. The high-kinetic-energy side of the valence band, which is predominantly of O $2p$ character,[29] can be fitted with a straight line that indicates the valence-band edge is at 3.8 eV below the Fermi level, which gives a 3.2 eV VBO. For the conduction band, which is primarily a mixture of Al $4s$ and $3p$ states, the Al_2O_3 band edge is fitted using two slopes: the first one from about 2 to 5 eV and the second one above 5 eV (see Fig. 6). After subtraction of the silicon background, the position of the conduction band with respect to the silicon midgap is 3.2 eV, giving a 2.7 eV CBO. The measured band gap for this Al_2O_3 film is 7.0 eV and is very different from the bulk value of 8 eV of the α-alumina, illustrating the importance of making these types of measurements on thin films, especially when the gap depends on the method of oxide film growth.[33] These values can be compared to other reported values (Table IV). Using the method outlined above, the electron affinity is measured to be 2.5 eV.

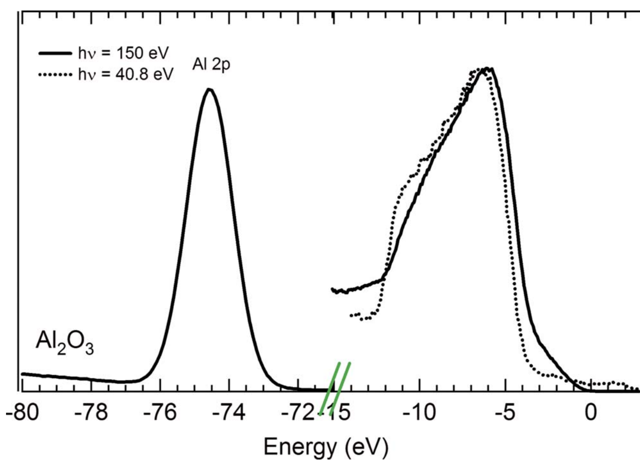

FIG. 11. (Color online) Al $2p$ core level and valence band measured at 150 eV photon energy (continuous line) and the valence band measured at 40.8 eV photon energy (dotted line). The zero of binding energy is referenced to the Si substrate Fermi level.

TABLE IV. Measured values for Al_2O_3 band gap and Al_2O_3-Si VBO and CBO in eV.

Method	Gap	VBO	CBO
XPS, energy loss[a]	6.95	3.75	2.08
XPS, energy loss[b]	6.52	3.03	2.37
XPS, energy loss[c]	6.7	2.9	2.7
IntPE[d]	6.2	2.95	2.15
SE[e]	6.26		
BEEM[f]			2.8
This work	7.0	3.2	2.5

[a]Reference 11.
[b]Reference 19.
[c]Reference 31.
[d]Reference 15.
[e]Reference 27.
[f]Reference 34.

IV. CONCLUSION

The experimental energy gaps and valence- and conduction-band offsets of different oxides with silicon and electron affinities, as well as the experimentally measured energy gap and electron affinity for silicon, are reported in Table V. As has been discussed in Sec. III for each oxide individually, the values obtained in this study using UPS and IPS are in good agreement with previously reported measurements. The differences among the experimental properties found in the literature can be explained either by the different experimental approaches or by the variability in sample preparation.

An important strength of this work compared to other previous measurements is that both the valence- and the conduction-band edges have been probed in the same UHV experimental chamber. Thus variations that are specific to particular samples such has rigid shifts due to dipole formation or defects state creation due to sample thermal treatment should be the same for both the occupied and unoccupied

TABLE V. Measured gap, VBO, and CBO with respect to silicon and χ in eV.

	Gap	VBO	CBO	χ
Si	1.1			4.1
SiO_2	8.9	4.5	3.3	1.3
HfO_2	5.7	2.7	1.9	2.5
$Hf_{0.7}Si_{0.3}O_2$	6.0	2.8	2.1	2.8
ZrO_2	5.5	2.7	1.7	2.7
Al_2O_3	7.0	3.2	2.7	2.5

states. The energy gap, as well as the electron affinity, can be directly obtained on the same samples, thus avoiding the use of literature values obtained from slightly different samples. For consistency, the synchrotron core-level spectroscopy can be compared to the UPS/IPS measurements, using as point of reference the valence-band spectra obtained in these two different experimental systems. The experimental techniques used in this work are particularly well adapted for the study of ultrathin films whose properties can be significantly altered from bulk properties.

One of the striking results of this study is that for all samples, with the exception of SiO_2, the Fermi level is measured close to the silicon conduction band, far from its expected position according to the silicon doping level. This indicates a strong downward band bending of the silicon band edges for all the high-$\kappa/SiO_2/Si$ samples. As it is observed only for high-κ stacks, the silicon band bending could be related to the high-κ/SiO_2 interface properties. It has been proposed that band bending of this sort could be explained by the presence of underoxidized and unpassivated silicon at the high-κ/SiO_2 interfaces as a consequence of the low-temperature deposition.[35,36] This work opens the possibility of studying *in situ*, passivation methods of these excess charges, as well as their effect on the band alignment across other high-κ gate stacks.

ACKNOWLEDGMENTS

We are grateful for the beam time allocation at the NSLS. The National Synchrotron Light Source, Brookhaven National Laboratory, is supported by the U.S. Department of Energy, Office of Science, Office of Basic Energy Sciences, under Contract No. DE-AC02-98CH10886. We would like to thank Lyudmila Goncharova for MEIS measurements, and we acknowledge the generous support of the SRC and the NSF.

[1] J. Robertson, J. Vac. Sci. Technol. B **18**, 1785 (2000).
[2] G. D. Wilk, R. M. Wallace, and J. M. Antony, J. Appl. Phys. **89**, 5243 (2001).
[3] This band diagram is not exact for several reasons. The vacuum level represented here is meaningful only for the high-κ material. We are also assuming that the bands are flat across the materials.
[4] D. Arena, F. Curti, and R. Bartynski, Surf. Sci. **369**, L117 (1996).
[5] E. Vescovo, H.-J. Kim, Q.-Y. Dong, G. Nintzel, D. Carlson, S. Hulbert, and N. V. Smith, Synchrotron Radiat. News **12**, 10 (1999).
[6] A. S. Foster, F. Lopez Gejo, A. L. Shluger, and R. M. Nieminen, Phys. Rev. B **65**, 174117 (2002).
[7] F. J. Himpsel, G. Hollinger, and R. A. Pollak, Phys. Rev. B **28**, 7014 (1983).
[8] R. Hofmann, W. A. Henle, and F. P. Netzer, Phys. Rev. B **44**, 3133 (1991).
[9] V. E. Henrich and P. A. Cox, *The Surface Science of Metal Oxides* (Cambridge University Press, Cambridge, 1994).
[10] R. P. Gupta, Phys. Rev. B **32**, 8278 (1985).
[11] S. Miyazaki, J. Vac. Sci. Technol. B **19**, 2212 (2001).
[12] J. Keister, J. Rowe, J. Kolodziej, H. Niimi, and T. Madey, J. Vac. Sci. Technol. B **17**, 1831 (1999).
[13] S. Sayan, E. Garfunkel, and S. Suzer, Appl. Phys. Lett. **80**, 2135 (2002).
[14] C. Fulton, G. Lucovsky, and R. Nemanich, J. Appl. Phys. **99**, 63708 (2006).
[15] V. Afanas'ev, M. Houssa, A. Stesmans, G. Adriaenssens, and M. Heyns, Microelectron. Eng. **59**, 335 (2001).
[16] G. L. Tan, M. F. Lemon, D. J. Jones, and R. H. French, Phys. Rev. B **72**, 205117 (2005).
[17] M. Ulrich, J. G. Hong, J. E. Rowe, G. Lucovsky, A.-Y. Chan, and T. E. Madey, J. Vac. Sci. Technol. B **21**, 1777 (2003).
[18] R. Puthenkovilakam and J. Chang, J. Appl. Phys. **96**, 2701 (2004).
[19] H. Y. Yu, M. F. Li, B. J. Cho, C. C. Yeo, M. S. Joo, D.-L. Kwong, J. S. Pan, C. H. Ang, J. Z. Zheng, and S. Ramanathan, Appl. Phys. Lett. **81**, 376 (2002).
[20] S. Sayan, T. Emge, E. Garfunkel, X. Zhao, L. Wielunski, R. Bartynski, D. Vanderbilt, J. Suehle, S. Suzer, and M. Banaszak-Holl, J. Appl. Phys. **96**, 7485 (2004).
[21] S. Toyoda, J. Okabayashi, H. Kumigashira, M. Oshima, K. Ono, M. Niwa, K. Usuda, and N. Hirashita, J. Electron Spectrosc. Relat. Phenom. **137-140**, 141 (2004).
[22] C. Fulton, G. Lucovsky, and R. Nemanich, Appl. Phys. Lett. **84**, 580 (2004).
[23] V. V. Afanas'ev, A. Stesmans, F. Chen, X. Shi, and S. A. Campbell, Appl. Phys. Lett. **81**, 1053 (2002).
[24] G. Lucovsky, J. Hong, C. Fulton, Y. Zou, R. Nemanich, and H. Ade, J. Vac. Sci. Technol. B **22**, 2132 (2004).
[25] N. Ikarashi and K. Manabe, J. Appl. Phys. **94**, 480 (2003).
[26] W. Zhu, T. Tamagawa, M. Gibson, T. Furakawa, and T. Ma, IEEE Electron Device Lett. **23**, 649 (2002).
[27] N. V. Nguyen, S. Sayan, I. Levin, J. R. Ehrstein, I. J. R. Baumvol, C. Driemeier, C. Krug, L. Wielunski, P. Y. Hung, and A. Diebold, J. Vac. Sci. Technol. A **23**, 1706 (2005).
[28] S. Sayan, R. Bartynski, X. Zhao, E. Gusev, D. Vanderbilt, M. Croft, H. Banaszak Holl, and E. Garfunkel, Phys. Status Solidi B **241**, 2246 (2004).
[29] J. Robertson, Rep. Prog. Phys. **69**, 327 (2006).
[30] R. Puthenkovilakam and J. Chang, Appl. Phys. Lett. **84**, 1353 (2004).
[31] H. Nohira, W. Tsai, W. Besling, E. Young, J. Petry, T. Conard, W. Vandervorst, S. De Gendt, M. Heyns, J. Maes, and M. Tuominen, J. Non-Cryst. Solids **303**, 83 (2002).
[32] L. Zhu, Q. Fang, G. He, M. Liu, X. Xu, and L. Zhang, Mater. Sci. Semicond. Process. **9**, 1025 (2006).
[33] V. V. Afanas'ev and A. Stesmans, J. Appl. Phys. **102**, 081301 (2007).
[34] R. Ludeke, M. T. Cuberes, and E. Cartier, Appl. Phys. Lett. **76**, 2886 (2000).
[35] J.-C. Lee, S.-J. Oh, M. Cho, C. S. Hwang, and R. Jung, Appl. Phys. Lett. **84**, 1305 (2004).
[36] J. L. Gavartin and A. L. Shluger, Microelectron. Eng. **84**, 2412 (2007).